

Laser-induced effects on the electronic features of graphene nanoribbons

Hernán L. Calvo, Pablo M. Perez-Piskunow, Stephan Roche, and Luis E. F. Foa Torres

Citation: [Applied Physics Letters](#) **101**, 253506 (2012); doi: 10.1063/1.4772496

View online: <http://dx.doi.org/10.1063/1.4772496>

View Table of Contents: <http://scitation.aip.org/content/aip/journal/apl/101/25?ver=pdfcov>

Published by the [AIP Publishing](#)

Articles you may be interested in

[Pure spin current induced by adiabatic quantum pumping in zigzag-edged graphene nanoribbons](#)

Appl. Phys. Lett. **104**, 183103 (2014); 10.1063/1.4873580

[Quasi-bound states and Fano effect in T-shaped graphene nanoribbons](#)

J. Appl. Phys. **114**, 153701 (2013); 10.1063/1.4824183

[Electronic properties of graphene nanoribbons with periodically hexagonal nanoholes](#)

J. Appl. Phys. **114**, 074307 (2013); 10.1063/1.4818615

[Fano effects in electron transport through an armchair graphene nanoribbon with one line defect](#)

J. Appl. Phys. **113**, 233701 (2013); 10.1063/1.4811438

[Scanning gate microscopy on a graphene nanoribbon](#)

Appl. Phys. Lett. **101**, 063101 (2012); 10.1063/1.4742862

An advertisement for Asylum Research Cypher AFMs. The background is dark blue with a stylized orange and yellow film strip on the left. The text is in white and orange. The Oxford Instruments logo is in the bottom right corner.

Not all AFMs are created equal

Asylum Research Cypher™ AFMs

There's no other AFM like Cypher

www.AsylumResearch.com/NoOtherAFMLikeIt

OXFORD
INSTRUMENTS

The Business of Science®

Laser-induced effects on the electronic features of graphene nanoribbons

Hernán L. Calvo,¹ Pablo M. Perez-Piskunow,² Stephan Roche,^{3,4} and Luis E. F. Foa Torres²

¹*Institut für Theorie der Statistischen Physik, RWTH Aachen University, D-52056 Aachen, Germany and JARA—Fundamentals of Future Information Technology*

²*Instituto de Física Enrique Gaviola (IFEG-CONICET) and FaMAF, Universidad Nacional de Córdoba, Ciudad Universitaria, 5000 Córdoba, Argentina*

³*CIN2(ICN-CSIC) and Universidad Autónoma de Barcelona, Catalan Institute of Nanotechnology, Campus UAB, 08193 Bellaterra (Barcelona), Spain*

⁴*ICREA, Institució Catalana de Recerca i Estudis Avançats, 08070 Barcelona, Spain*

(Received 29 September 2012; accepted 3 December 2012; published online 18 December 2012)

We study the interplay between lateral confinement and photon-induced processes on the electronic properties of illuminated graphene nanoribbons. We find that by tuning the device setup (edges geometries, ribbon width, and polarization direction), a laser with frequency Ω may either not affect the electronic structure, or induce bandgaps or depletions at $\pm\hbar\Omega/2$, and/or at other energies not commensurate with half the photon energy. Similar features are also observed in the dc conductance, suggesting the use of the polarization direction to switch on and off the graphene device. Our results could guide the design of novel types of optoelectronic nano-devices.

© 2012 American Institute of Physics. [<http://dx.doi.org/10.1063/1.4772496>]

The extraordinary properties of graphene^{1–3} led to an unprecedented narrowing in the expected gap between the understanding of phenomena and the development of disruptive applications.¹ Though originally focused mainly on pure electronic, mechanical, or optical properties, much attention is now devoted to the interplay between these variables.⁴ Graphene optoelectronics,^{4–10} in particular, is one of the most active and promising fields with flagship applications including energy harvesting devices⁶ and novel plasmonic properties.^{8,11}

Recently, the captivating possibility of controlling the electronic properties of graphene through simple illumination with a laser field^{12,13} has been re-examined through atomistic calculations,¹⁴ calculations of the optical response,^{15,16} and proposals for tuning the topological properties of the underlying photon-induced states,^{17–20} among other interesting issues.^{21–26} The basic idea is that laser illumination may couple states on each side of the charge neutrality point inducing a bandgap at $\pm\hbar\Omega/2$, if the field intensity and frequency are appropriately tuned. This non-adiabatic and non-perturbative effect relies crucially on the low dimensionality and peculiar electronic structure of graphene and has attracted much recent attention.^{17–20} Notwithstanding, most of these predictions were restricted to bulk graphene. One may wonder about the possible consequences of reduced dimensionality and quantum confinement.

Here, we address the effects of laser illumination on graphene nanoribbons and show that lateral confinement plays a crucial role: tuning the sample size and the direction between the laser polarization relative to the sample edges, linearly polarized light may or not induce bandgaps or depletions in the density of states and the conductance spectra. Strikingly, for finite size samples, these features may appear at energies different from integer multiples of $\pm\hbar\Omega/2$. This is in stark contrast with bulk graphene where the electrical response is insensitive to the linear polarization direction. Our results fill the gap in the understanding of the laser-induced control of

the electrical response and may guide the design of experiments on optoelectronic devices.

Hamiltonian model and solution scheme. We consider an infinite graphene nanoribbon illuminated by a laser only in a finite region of length L and perpendicular to it (as shown schematically in Fig. 1(a)). Electrons in the graphene ribbon are modeled through a nearest neighbours π -orbitals Hamiltonian^{3,27} $H_e = \sum_i E_i c_i^\dagger c_i - \sum_{\langle i,j \rangle} [\gamma_{ij} c_i^\dagger c_j + \text{H.c.}]$, where c_i^\dagger and c_i are the electronic creation and annihilation operators at site i , E_i are the on-site energies and γ_{ij} the nearest-neighbors carbon-carbon hopping amplitudes, which are taken equal to $\gamma_0 = 2.7\text{eV}$.³ Radiation is described through a time-dependent electric field \mathbf{E} . By choosing a gauge such that $\mathbf{E} = -\partial\mathbf{A}/\partial t$, where \mathbf{A} is the vector potential, the hopping matrix elements acquire a time-dependent phase according to: $\gamma_{ij} = \gamma_0 \exp(i\frac{2\pi}{\Phi_0} \int_{\mathbf{r}_i}^{\mathbf{r}_j} \mathbf{A}(t) \cdot d\mathbf{r})$, where Φ_0 is the magnetic flux quantum.

Retaining *non-perturbative* and *non-adiabatic* corrections to the electrical response is crucial for the results presented hereafter. In this regime, Floquet theory provides an appropriate framework. An efficient solution using this scheme is used to obtain the average density of states and the dc component of the conductance, which is computed from the inelastic transmission probabilities in Floquet space.²⁸ The interested reader may find further generalities of the method in Refs. 28 and 29, while more technical details will be published elsewhere.³⁰ For a periodic modulation of the hoppings, the spectral and transport properties can be derived from the so-called Floquet Hamiltonian: $H_F = H_e - i\hbar\partial/\partial t$. Such Hamiltonian has a time-independent representation in the Floquet space, which is the direct product between the usual Hilbert space and the space of time-periodic functions with the same period as the Hamiltonian H_e .^{28,31} Therefore, on top of the k label, our states have a second label n , which indicates the number n of photon excitations in the system. In the absence of radiation, the quasi-energies spectrum of H_F is given by $\varepsilon(\mathbf{k}, n) = \varepsilon_0(\mathbf{k}) + n\hbar\Omega$ ($\varepsilon_0(\mathbf{k})$ is the spectrum of H_e).

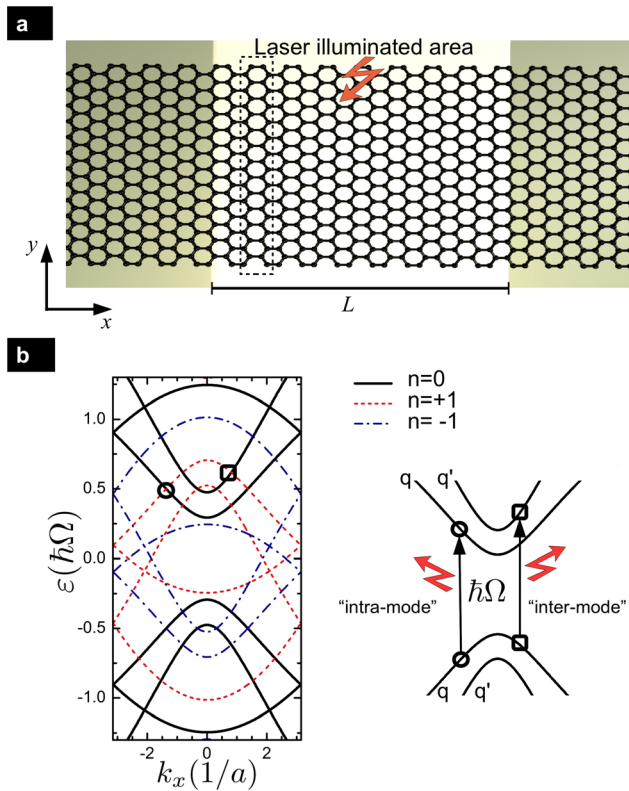


FIG. 1. (a) Scheme of the considered setup: A graphene nanoribbon illuminated by a mid-infrared laser within a finite region of length L . The unit cell for the case of an armchair ribbon is marked with a rectangle (dashed line) and contains $4N$ atoms in the notation used in the text. (b) Floquet quasi-energy dispersion for a small ribbon ($N=2$). For the sake of better visualization, we show the quasi-energy spectrum without radiation (this allows to better distinguish the crossings between levels) and choose arbitrary frequency and intensity values. More realistic results are shown in Figs. 2 and 3. The scheme on the right shows the electronic states for two of such transitions.

Electronic properties of irradiated graphene nanoribbons. The first question concerns the response of graphene nanoribbons to a linearly polarized laser excitation. While in the bulk limit, both the conductance and the density of states (DOS) are independent on the polarization direction, the picture turns out to change radically in confined geometries.

Figure 2 shows the average density of states as a function of the Fermi energy for a frequency in the mid-infrared regime ($\hbar\Omega = 140$ meV). Two different armchair nanoribbons widths and polarizations are chosen: $N=130$ (a) and (b), $N=129$ (c) and (d); and linear polarization along the x (a) and (c) and y (b) and (d) directions. For $N=130$, one sees the appearance of strong depletions at $\pm\hbar\Omega/2$. These depletions are located at the same energy as the ones for the bulk system¹⁴ and correspond to the excitation of an electron between the conjugate states at $\pm\hbar\Omega/2$. In striking contrast, the DOS is restored at $\pm\hbar\Omega/2$ for y -polarized laser, whereas features occur at energies incommensurate with $\hbar\Omega$.

The DOS for the ribbon with $N=129$ (c and d) also exhibit a laser-induced fragmentation of the spectrum. In this case, the observation of fully depleted energy regions (bandgap) at $\pm\hbar\Omega/2$. One observes that by increasing the laser intensity, some DOS modifications are further enhanced (see for instance, the DOS depletion around $\hbar\Omega/2$ for Fig. 2(a)), complemented by the emergence of fine struc-

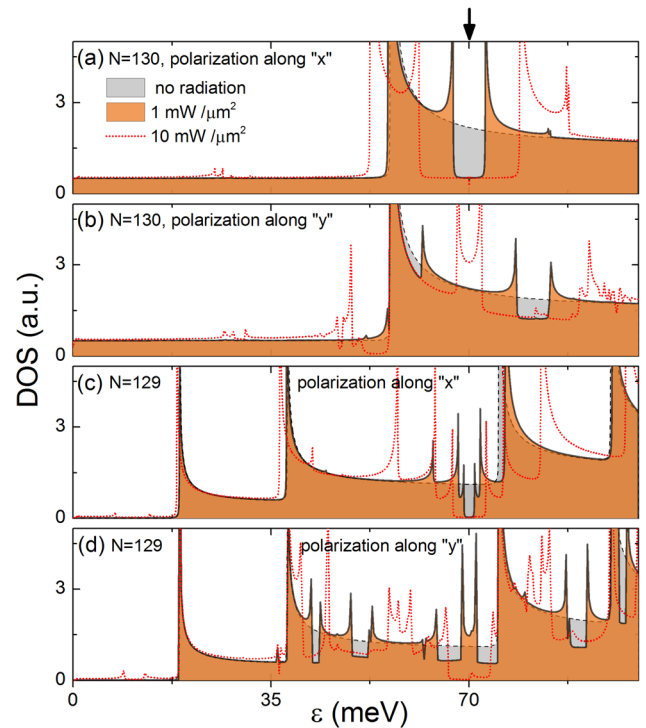


FIG. 2. Average density of states for armchair graphene nanoribbons with $N=130$ ((a) and (b)) and $N=129$ ((c) and (d)) for two values of the laser power P : $1 \text{ mW}/\mu\text{m}^2$ (solid black line with orange shaded area) and $10 \text{ mW}/\mu\text{m}^2$ (dotted red line). Panels a and c ((b) and (d)) are for polarization along the x direction (y direction). The energy corresponding to $\hbar\Omega/2$ is marked with an arrow for reference in the top of the panel. The DOS in absence of radiation is also shown for comparison (dashed lines, grey shaded area).

ture. Figure 3 shows the dc conductance as a function of the Fermi energy position for the case shown in Fig. 2. Here, we see that the depletions in the DOS yield the same conductance fingerprints. One can see that *switching the polarization direction may produce a marked on-off ratio if the Fermi energy is appropriately tuned*.

To rationalize these differences, it is instructive to write H_e in a basis of independent transversal channels or modes as discussed in Refs. 33 and 34. In the absence of radiation, the Floquet spectrum of the system is just the sum of the contributions from each of the modes $\varepsilon_0(\mathbf{k})$ plus their Floquet replicas: $\varepsilon(\mathbf{k}, n) = \varepsilon_0(\mathbf{k}) + n\hbar\Omega$. An illustration for a very small system is shown in Fig. 1(b), each mode contains an electron and a hole branch. At the crossings between the different lines, one may expect stronger effects of the radiation (if it provides the necessary coupling between the corresponding states).

From the Floquet spectrum in Fig. 1(b), one can see that there are two kind of crossings: the ones that connect an electronic (hole) state with a hole (electron) state belonging to the same mode plus or minus an integer number of photons (like the one marked with an open circle); and the ones that connect states in different modes (as the one marked with an open square in Fig. 1(b)). In such cases, a non-vanishing matrix element of the Floquet Hamiltonian will give intra and inter-mode transitions, respectively. Given the electron-hole symmetry of the spectrum, intra-mode transitions always connect states, which are symmetric relative to

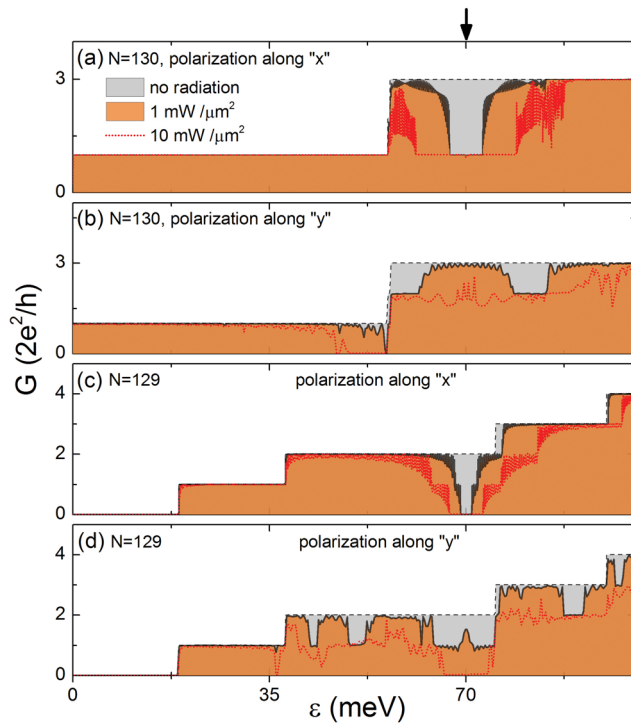


FIG. 3. DC conductance for armchair graphene nanoribbons with $N = 130$ ((a) and (b)) and $N = 129$ ((c) and (d)). Panels a and c ((b) and (d) are for polarization along the x direction (y direction).

the Dirac point, i.e., integer multiples of $\pm\hbar\Omega/2$. On other hand, inter-mode transitions always couple states which are not symmetrically located from the Dirac point, as can be seen on Fig. 1(b). A scheme showing these two type of transitions is shown in Fig. 1(b).

For armchair graphene nanoribbons, it turns out that a laser with linear polarization along the transport direction (x) does not mix these transversal modes, leading to features in the density of states *only* at $\pm\hbar\Omega/2$ as can be seen in Fig. 1(b). On the other hand, calculation of the matrix elements shows that when the polarization is along y , inter-mode processes are allowed and intra-mode ones are forbidden. Depletions and gaps develop at the crossing between Floquet states corresponding to *different* modes leading to the features observed in Figs. 2(b) and 2(c).

A complementary approach to this problem is possible by using the k,p model, which could be accurate enough for medium-sized ribbons.³² A careful analysis shows consistent results: inter-mode processes lead to gaps/depletions located away from $\pm\hbar\Omega/2$ while polarization along y suppresses the depletions at $\pm\hbar\Omega/2$. In the bulk limit, as the energy difference between subbands gets smaller, the crossings between Floquet states accumulate close to $\pm\hbar\Omega/2$ leading to the same behavior for both polarizations (along x and y). A flavor of this can be seen in the red dotted lines in Figs. 2(b) and 2(c): The two depletions seen in Fig. 2(d) black line merge when increasing the laser power.

Another interesting feature is that the metallic modes/subbands in armchair ribbons are quite insensitive to the radiation (as seen in Figs. 2 and 3). Hence, very small metallic armchair ribbons containing only one transport channel within the energy range of interest will not experience rele-

vant changes in their electronic properties. We emphasize that this is a peculiar property of armchair graphene nanoribbons.³⁰

Figures 2 and 3 correspond to a laser frequency in the mid-infrared, which gives an optimum playground to test these predictions in the laboratory. Going to higher frequencies may help to achieve device miniaturization but the size of the gaps and depletions at constant laser power diminishes, whereas at very low frequencies (THz), the gaps further decrease. Experiments would require temperatures below 20 K for $P \simeq 1 \text{ mW}/\mu\text{m}^2$.

In summary, we show that the interplay between photon-induced inelastic processes and lateral confinement in graphene nanoribbons leads to diverse modifications in the band structure and transport properties not evident in the bulk limit. In the case of moderate sized nanoribbons (ca. 10 nm), the careful tuning of the polarization direction may widen the opportunities for achieving control of the electrical response in optoelectronic devices.

We acknowledge support by SeCyT-UNC, ANPCyT-FonCyT (Argentina). L.E.F.F.T. acknowledges the support from the Alexander von Humboldt Foundation and ICTP-Trieste, as well as discussions with G. Usaj.

- ¹A. K. Geim, *Science* **324**, 1934 (2009); A. K. Geim and K. S. Novoselov, *Nature Mater.* **6**, 183 (2007).
- ²A. H. Castro Neto, F. Guinea, N. M. R. Peres, K. S. Novoselov, and A. K. Geim, *Rev. Mod. Phys.* **81**, 109 (2009).
- ³S. M.-M. Dubois, Z. Zanolli, X. Declercq, and J.-C. Charlier, *Eur. Phys. J. B* **72**, 1 (2009); J.-C. Charlier, X. Blase, and S. Roche, *Rev. Mod. Phys.* **79**, 677 (2007).
- ⁴F. Bonaccorso, Z. Sun, T. Hasan, and A. C. Ferrari, *Nature Photon.* **4**, 611 (2010).
- ⁵F. Xia, T. Mueller, Y.-m. Lin, A. Valdes-Garcia, and P. Avouris, *Nat. Nanotechnol.* **4**, 839 (2009).
- ⁶N. M. Gabor, J. C. W. Song, Q. Ma, N. L. Nair, T. Taychatanapat, K. Watanabe, T. Taniguchi, L. S. Levitov, and P. Jarillo-Herrero, *Science* **334**, 648 (2011).
- ⁷J. Karch, C. Drexler, P. Olbrich, M. Fehrenbacher, M. Hirmer, M. M. Glazov, S. A. Tarasenko, E. L. Ivchenko, B. Birkner, J. Eroms *et al.*, *Phys. Rev. Lett.* **107**, 276601 (2011).
- ⁸F. H. L. Koppens, D. E. Chang, and F. J. Garcia de Abajo, *Nano Lett.* **11**, 3370 (2011).
- ⁹L. Ren, C. L. Pint, L. G. Booshehri, W. D. Rice, X. Wang, D. J. Hilton, K. Takeya, I. Kawayama, M. Tonouchi, R. H. Hauge, and J. Kono, *Nano Lett.* **9**, 2610 (2009).
- ¹⁰J. W. McIver, D. Hsieh, H. Steinberg, P. Jarillo-Herrero, and N. Gedik, *Nat. Nanotechnol.* **7**, 96 (2012).
- ¹¹J. Chen, M. Badioli, P. Alonso-Gonzalez, S. Thongrattanasiri, F. Huth, J. Osmond, M. Spasenovic, A. Centeno, A. Pesquera, Ph. Godignon, A. Zurutuza Elorza, N. Camara, F. J. Garcia de Abajo, R. Hillenbrand, and F. H. L. Koppens, "Optical nano-imaging of gate-tunable graphene plasmons," *Nature* (to be published).
- ¹²S. V. Syzranov, M. V. Fistul, and K. B. Efetov, *Phys. Rev. B* **78**, 045407 (2008).
- ¹³T. Oka and H. Aoki, *Phys. Rev. B* **79**, 081406 (2009).
- ¹⁴H. L. Calvo, H. M. Pastawski, S. Roche, and L. E. F. Foa Torres, *Appl. Phys. Lett.* **98**, 232103 (2011).
- ¹⁵Y. Zhou and M. W. Wu, *Phys. Rev. B* **83**, 245436 (2011).
- ¹⁶M. Busl, G. Platero, and A.-P. Jauho, *Phys. Rev. B* **85**, 155449 (2012).
- ¹⁷T. Kitagawa, T. Oka, A. Brataas, L. Fu, and E. Demler, *Phys. Rev. B* **84**, 235108 (2011).
- ¹⁸Z. Gu, H. A. Fertig, D. P. Arovas, and A. Auerbach, *Phys. Rev. Lett.* **107**, 216601 (2011).
- ¹⁹B. Dóra, J. Cayssol, F. Simon, and R. Moessner, *Phys. Rev. Lett.* **108**, 056602 (2012).
- ²⁰E. Suárez Morell and L. E. F. Foa Torres, *Phys. Rev. B* **86**, 125449 (2012).
- ²¹D. S. L. Abergel and T. Chakraborty, *Appl. Phys. Lett.* **95**, 062107 (2009).

- ²²O. V. Kibis, *Phys. Rev. B* **81**, 165433 (2010).
- ²³S. E. Savelev and A. S. Alexandrov, *Phys. Rev. B* **84**, 035428 (2011).
- ²⁴A. Iurov, G. Gumbs, O. Roslyak, and D. Huang, *J. Phys.: Condens. Matter* **24**, 015303 (2012).
- ²⁵J.-T. Liu, F.-H. Su, H. Wang, and X.-H. Deng, *New J. Phys.* **14**, 013012 (2012).
- ²⁶P. San-Jose, E. Prada, H. Schomerus, and S. Kohler, *Appl. Phys. Lett.* **101**, 153506 (2012).
- ²⁷R. Saito, G. Dresselhaus, and M. S. Dresselhaus, *Physical Properties of Carbon Nanotubes* (Imperial College Press, London, 1998).
- ²⁸S. Kohler, J. Lehmann, and P. Hänggi, *Phys. Rep.* **406**, 379 (2005).
- ²⁹L. E. F. Foa Torres, *Phys. Rev. B* **72**, 245339 (2005).
- ³⁰H. L. Calvo, P. Perez Piskunow, H. M. Pastawski, S. Roche, and L. E. F. Foa Torres, “Non-perturbative laser effects on the electrical properties of graphene nanoribbons” (unpublished).
- ³¹J. H. Shirley, *Phys. Rev.* **138**, B979 (1965); H. Sambe, *Phys. Rev. A* **7**, 2203 (1973).
- ³²L. Brey, H. A. Fertig, *Phys. Rev. B* **73**, 235411 (2006); P. Marconcini and P. Maccuci, *Riv. Nuovo Cimento* **34**, 489 (2011).
- ³³C. G. Rocha, L. E. F. Foa Torres, and G. Cuniberti, *Phys. Rev. B* **81**, 115435 (2010).
- ³⁴P. Zhao and J. Guo, *J. Appl. Phys.* **105**, 034503 (2009).